JOURNAL OF COMPUTATIONAL PHYSICS 22, 74–86 (1976)

A Second-Order, Time Integration Scheme for Calculating Stratified Incompressible Flows

ROBERT K. -C. CHAN

Jaycor, Del Mar, California 92014

Received September 8, 1975

An explicit, second-order, two-level, time-integration scheme for calculating density-stratified incompressible flows is described. It is demonstrated that this method is stable for long-term integration with respect to time and that excellent conservation of mass, momentum, and energy has been achieved. Moreover, the small error that could occur in the total energy is nonaccumulative. The time-step splitting error, encountered in many second-order time schemes, does not arise in the present method when all the initial conditions are consistent with the implications of the basic equations of motion.

1. INTRODUCTION

A major consideration in studying the generation and propagation of internal gravity waves in a density stratified liquid, as in oceanic situations, is the energetic content of the wave system. Consequently, computational accuracy in terms of energy conservation, in addition to the conservation of mass and momentum, must be achieved when devising a finite-difference method for such applications. There exist a class of semiconservative finite-difference schemes [1–4] which conserve energy only in the absence of time-differencing errors [5]. In fact, difference schemes that semiconserve energy but that are unstable when leapfrog time-differencing is used have been reported by Kreiss and Oliger [6]. The key in these semiconservation methods is in the careful construction of the difference representation of the convection terms. In the present application, however, the nonlinear convection terms play a minor role as the internal gravity waves are maintained primarily by the balance between local accelerations and the pressure gradient. Consequently, as the present author has found, whether one uses an energy conserving scheme for the convection terms has little effect on the solution of the present problem. Here they key obviously lies in time-differencing.

The semiconservative scheme of Piacsek and Williams [4] has been used with a three-level leapfrog time differencing by Dugan, *et al.*[7], to study the collapse of a mixed region in a density stratified fluid. They reported the occurrence of "compu-

tational modes," presumably the time-step splitting wherein two unrelated, disjoint solutions develop which alternate at each time step [8]; the computational modes were suppressed by periodically averaging the numerical solution over adjacent time steps to avoid serious deviations from the correct solution. Their sample calculation was performed for 14 Brunt–Väisälä periods. Although the total energy was conserved to within 5% throughout that calculation, the most unsettling fact is that the total energy increased almost linearly at the rate of 0.31% per Brunt–Väisälä period, as can be seen in Fig. 2 of their work. It seems that the solution might eventually produce significant error in total energy if the computation was continued much longer. Thus, the absolute quadratic conservation property of the difference scheme for the convection terms has been overwhelmed by the property of the leapfrog time differencing.

In this paper, we describe an explicit, second-order, two-level, time-integration scheme which has been found by extensive experiments to be free of the difficulties mentioned above. Specifically, this method produces nonsystematic error in total energy which remains less than 1% throughout each run, in sharp contrast with the accumulative error reported in [7]. Also, time-step splitting error does not occur in the present procedure if a *consistent* set of initial values are prescribed at the initial time level $t = 0$. Thus, unlike the three-level leapfrog method, which raises a first-order continuum equation in time to a second-order difference equation in time, one need not worry about special starting procedures and their implications on the solution [9]. Results of sample calculations are included to illustrate the properties of the present technique.

2. The Solution Procedure

Consider the two-dimensional, time-dependent motion of a density stratified fluid, for which the stable equilibrium density profile ρ_0 is a function of the vertical coordinate y only. Let (x, y) be the rectangular cartesian coordinates and (u, v) the corresponding components of the fluid velocity. With the usual Boussinesq approximation [10], namely, that the effect of density variation need only be accounted for in the buoyancy term, the equations of motion for an inviscid, incompressible fluid are

$$u_t = -\{(u^2)_x + (uv)_y + \phi_x\} \tag{1}$$

$$v_t = -\{(uv)_x + (v^2)_y + (g/\rho^*)\,\rho' + \phi_y\} \tag{2}$$

$$\rho_t' = -\{(u\rho')_x + (v\rho')_y + (\rho_0)_y v\} \tag{3}$$

$$u_x + v_y = 0 \tag{4}$$

where $\phi \equiv p/\rho^*$ (p is the fluid pressure less the hydrostatic contribution and ρ^* is a constant, reference density, e.g., the average density of the fluid considered), g is

the gravitational acceleration, and $\rho' \equiv \rho(x, y, t) - \rho_0(y)$ is the density deviation from the undisturbed value. In the equations above, subscripts imply partial differentiation.

The convection terms in Eqs. (1)–(3) have been written in conservation form so that the linear quantities u, v, and ρ' are rigorously conserved when they are replaced by a suitable difference scheme. Although a difference scheme with the property of conserving quadratic quantities absolutely [4], i.e., in the absence of time-differencing error, could be used to calculate the convection terms, we use the usual central difference for the reason that the physical system to be studied is governed by the balance between the local acceleration and the pressure gradient. In such a system, truncation errors in convection terms have negligible effects on the solution, but the presence of linear "stiff terms," i.e., ρ' in Eq. (2) and v in Eq. (3), requires a careful treatment in time integration. Experience shows that a simplistic, explicit, first-order, forward time scheme is unstable, while implicit treatment of the stiff terms dissipates the energy artificially. Since the three-level leapfrog time-differencing scheme has the difficulties discussed in the previous section, we are led to look for an alternative way of formulating a second-order time scheme.

Differentiating each term in Eqs. (1)–(3) with respect to the time t, we have

$$u_{tt} = -(2uu_t)_x - (u_t v + uv_t)_y - \phi_{xt} \tag{5}$$

$$v_{tt} = -(u_t v + uv_t)_x - (2vv_t)_y - (g/\rho^*)\,\rho_t' - \phi_{yt} \tag{6}$$

$$\rho'_{tt} = -(u_t\rho' + u\rho_t')_x - (v_t\rho' + v\rho_t')_y - (\rho_0)_y\, v_t\,. \tag{7}$$

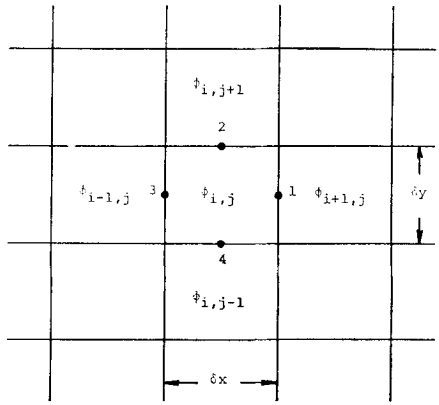

FIG. 1. Position of flow variables; (1) $u_{i+(1/2),j}$ (2) $v_{i,j+(1/2)}$ and $\rho'_{i,j+(1/2)}$ (3) $u_{i-(1/2),j}$ (4) $v_{i,j-(1/2)}$ and $\rho'_{i,j-(1/2)}$.

To implement a finite-difference solution procedure, the fluid domain of interest is divided into many rectangular subregions, or cells, as shown in Fig. 1. Each cell has the dimensions δx by δy. Associated with each cell, ϕ is defined at the cell center, u is evaluated at the midpoint of the left and right edges of the cell, and v, as well as ρ', is defined at the midpoint of the top and bottom edges of the cell. Simple averaging is used to obtain values where they are not formally defined.

Since we have an initial-value problem, the values of u, v, ϕ, and ρ' must be given at their points of definition at some initial time $t = 0$. Subsequently, the finite-difference representations of the governing equations are used to advance these quantities with respect to time. Let f^n be any of these quantities evaluated at the time $t = t^n$ and f^{n+1} be the same quantity at $t = t^{n+1}$, where $t^{n+1} - t^n = \delta t$ is the positive time increment. Then, using Taylor's series expansion in δt we have

$$f^{n+1} = f^n + \delta t(f_t)^n + (\delta t^2/2!)(f_{tt})^n + O(\delta t^3) \tag{8}$$

which provides the basis of an explicit, second-order, time-integration procedure. A similar temporal expansion was used by Gazdag [11] who related the temporal derivatives to spatial derivatives. Serious difficulties arise in Gazdag's approach, because the time-expansion process adds requirements for additional boundary conditions on spatial derivatves which are not present in the original differential equations. In the present approach, instead of translating temporal derivatives into spatial derivatives, the quantities u_t, v_t, and ρ_t' are regarded as auxiliary dependent variables for which appropriate boundary conditions can be found naturally from the physical problem. Discussion of boundary conditions will be given later. In the mesh system shown in Fig. 1, u_t, v_t, and ρ_t' are defined at the same locations as are u, v, and ρ', respectively.

To get to the heart of the computational procedure, it is best to examine the finite-difference equations in detail. Suppose central difference is used for evaluating spatial derivatives, e.g., ϕ_x at the location $(i + (1/2), j)$ (Fig. 1) is written as

$$(\phi_x)^n_{i+(1/2),j} = \frac{\phi^n_{i+1,j} - \phi^n_{i,j}}{\delta x}. \tag{9}$$

The mixed derivatives ϕ_{xt} and ϕ_{yt}, appearing in Eqs. (5) and (6), are represented by

$$\begin{aligned}(\phi_{xt})^n_{i+(1/2),j} &= [(\phi_x)^{n+1}_{i+(1/2),j} - (\phi_x)^n_{i+(1/2),j}]/\delta t + O(\delta t)\\ (\phi_{yt})^n_{i,j+(1/2)} &= [(\phi_y)^{n+1}_{i,j+(1/2)} - (\phi_y)^n_{i,j+(1/2)}]/\delta t + O(\delta t).\end{aligned} \tag{10}$$

It can be shown by Taylor series expansion that these approximations for ϕ_{xt} and ϕ_{yt} contain truncation errors of the order δt in time. However, when these expressions are used in Eqs. (5) and (6), which are in turn substituted into Eq. (8),

where f is replaced with u or v, these truncation errors are of the order $(\delta t)^3$, owing to the factor $(\delta t)^2/2!$. Thus, with Eq. (10) the formal accuracy of the present method is consistently second-order in δt for all variables involved.

Substituting Eqs. (1) and (5) into Eq. (8), for the location $(i + (1/2), j)$, we get

$$\begin{aligned} u^{n+1}_{i+(1/2),j} = {} & u^n_{i+(1/2),j} + \delta t(u_t)^n_{i+(1/2),j} - (\delta t^2/2)\{[2u^n_{i+1,j}(u_t)^n_{i+1,j} - 2u^n_{i,j}(u_t)^n_{i,j}]/\delta x \\ & + [(u_t)^n_{i+(1/2),j+(1/2)}v^n_{i+(1/2),j+(1/2)} + u^n_{i+(1/2),j+(1/2)}(v_t)^n_{i+(1/2),j+(1/2)} \\ & - (u_t)^n_{i+(1/2),j-(1/2)}v^n_{i+(1/2),j-(1/2)} - u^n_{i+(1/2),j-(1/2)}(v_t)^n_{i+(1/2),j-(1/2)}]/\delta y\} \\ & + (\delta t/2)(\phi^n_{i+1,j} - \phi^n_{i,j})/\delta x - (\delta t/2)(\phi^{n+1}_{i+1,j} - \phi^{n+1}_{i,j})/\delta x \end{aligned} \tag{11}$$

where

$$\begin{aligned} (u_t)^n_{i+(1/2),j} = {} & -\{(u^{n^2}_{i+1,j} - u^{n^2}_{i,j})/\delta x + (u^n_{i+(1/2),j+(1/2)}v^n_{i+(1/2),j+(1/2)} \\ & - u^n_{i+(1/2),j-(1/2)}v^n_{i+(1/2),j-(1/2)})/\delta y + (\phi^n_{i+1,j} - \phi^n_{i,j})/\delta x\}. \end{aligned} \tag{12}$$

Similarly, we can combine Eqs. (2), (6), and (8) to give

$$\begin{aligned} v^{n+1}_{i,j+(1/2)} = {} & v^n_{i,j+(1/2)} + \delta t(v_t)^n_{i,j+(1/2)} \\ & - (\delta t^2/2)\{[(u_t)^n_{i+(1/2),j+(1/2)}v^n_{i+(1/2),j+(1/2)} + u^n_{i+(1/2),j+(1/2)}(v_t)^n_{i+(1/2),j+(1/2)} \\ & - (u_t)^n_{i-(1/2),j+(1/2)}v^n_{i-(1/2),j+(1/2)} - u^n_{i-(1/2),j+(1/2)}(v_t)^n_{i-(1/2),j+(1/2)}]/\delta x \\ & + [2v^n_{i,j+1}(v_t)^n_{i,j+1} - 2v^n_{i,j}(v_t)^n_{i,j}]/\delta y + (g/\rho^*)(\rho_t')^n_{i,j+(1/2)}\} \\ & + (\delta t/2)(\phi^n_{i,j+1} - \phi^n_{i,j})/\delta y - (\delta t/2)(\phi^{n+1}_{i,j+1} - \phi^{n+1}_{i,j})/\delta y \end{aligned} \tag{13}$$

where

$$\begin{aligned} (v_t)^n_{i,j+(1/2)} = {} & -\{(u^n_{i+(1/2),j+(1/2)}v^n_{i+(1/2),j+(1/2)} - u^n_{i-(1/2),j+(1/2)}v^n_{i-(1/2),j+(1/2)})/\delta x \\ & + (v^{n^2}_{i,j+1} - v^{n^2}_{i,j})/\delta y + (g/\rho^*)(\rho')^n_{i,j+(1/2)} + (\phi^n_{i,j+1} - \phi^n_{i,j})/\delta y\}. \end{aligned} \tag{14}$$

Also, Eqs. (3), (7), and (8) give

$$\begin{aligned} (\rho')^{n+1}_{i,j+(1/2)} = {} & (\rho')^n_{i,j+(1/2)} + \delta t(\rho_t')^n_{i,j+(1/2)} \\ & - (\delta t^2/2)\{[(u_t)^n_{i+(1/2),j+(1/2)}\rho'^n_{i+(1/2),j+(1/2)} + u^n_{i+(1/2),j+(1/2)}(\rho_t')^n_{i+(1/2),j+(1/2)} \\ & - (u_t)^n_{i-(1/2),j+(1/2)}\rho'^n_{i-(1/2),j+(1/2)} - u^n_{i-(1/2),j+(1/2)}(\rho_t')^n_{i-(1/2),j+(1/2)}]/\delta x \\ & + [(v_t)^n_{i,j+1}\rho'^n_{i,j+1} + v^n_{i,j+1}(\rho_t')^n_{i,j+1} - (v_t)^n_{i,j}\rho'^n_{i,j} - v^n_{i,j}(\rho_t')^n_{i,j}]/\delta y \\ & + [(\rho_0)_y]_{i,j+(1/2)}(v_t)^n_{i,j+(1/2)}\} \end{aligned} \tag{15}$$

where

$$(\rho_t')^n_{i,j+(1/2)} = -\{(u^n_{i+(1/2),j+(1/2)}\rho'^n_{i+(1/2),j+(1/2)} - u^n_{i-(1/2),j+(1/2)}\rho'^n_{i-(1/2),j+(1/2)})/\delta x$$

$$+ (v^n_{i,j+1}\rho'^n_{i,j+1} - v^n_{i,j}\rho'^n_{i,j})/\delta y + [(\rho_0)_y]_{i,j+(1/2)}v^n_{i,j+(1/2)}\}. \tag{16}$$

Finally, Eq. (4) is written in the familiar form

$$(u^{n+1}_{i+(1/2),j} - u^{n+1}_{i-(1/2),j})/\delta x + (v^{n+1}_{i,j+(1/2)} - v^{n+1}_{i,j-(1/2)})/\delta y = 0. \tag{17}$$

As in the MAC class of methods [12], a Poisson equation for the new pressure ϕ^{n+1} can be obtained by the following procedure. First, Eqs. (11) and (13) are cast in the form

$$\begin{aligned}
u^{n+1}_{i+(1/2),j} &= \tilde{u}_{i+(1/2),j} - (\delta t/2)(\phi^{n+1}_{i+1,j} - \phi^{n+1}_{i,j})/\delta x \\
u^{n+1}_{i-(1/2),j} &= \tilde{u}_{i-(1/2),j} - (\delta t/2)(\phi^{n+1}_{i,j} - \phi^{n+1}_{i-1,j})/\delta x \\
v^{n+1}_{i,j+(1/2)} &= \tilde{v}_{i,j+(1/2)} - (\delta t/2)(\phi^{n+1}_{i,j+1} - \phi^{n+1}_{i,j})/\delta y \\
v^{n+1}_{i,j-(1/2)} &= \tilde{v}_{i,j-(1/2)} - (\delta t/2)(\phi^{n+1}_{i,j} - \phi^{n+1}_{i,j-1})/\delta y
\end{aligned} \tag{18}$$

where the tilde quantities depend on information at the nth time level only. Substituting these expressions into Eq. (17), we obtain the desired Poisson equation:

$$(\phi^{n+1}_{i+1,j} - 2\phi^{n+1}_{i,j} + \phi^{n+1}_{i-1,j})/(\delta x)^2 + (\phi^{n+1}_{i,j+1} - 2\phi^{n+1}_{i,j} + \phi^{n+1}_{i,j-1})/(\delta y)^2$$

$$= (2/\delta t)[(\tilde{u}_{i+(1/2),j} - \tilde{u}_{i-(1/2),j})/\delta x + (\tilde{v}_{i,j+(1/2)} - \tilde{v}_{i,j-(1/2)})/\delta y]. \tag{19}$$

Each computation cycle consists of the following steps:

1. From the known u^n, v^n, ρ'^n, and ϕ^n, calculate $(u_t)^n$, $(v_t)^n$, and $(\rho_t')^n$ according to Eqs. (12), (14), and (16), respectively.

2. Calculate $\tilde{u}$ and $\tilde{v}$, which can be deduced from comparing Eq. (18) with Eqs. (11) and (13).

3. Calculate and store the source term, i.e., the right side, of Eq. (19). Then, solve the pressure field $\phi^{n+1}_{i,j}$ by using either a direct solver or some iterative procedure [8].

4. Obtain final values for u^{n+1} and v^{n+1}, using Eq. (18).

5. Calculate $(\rho')^{n+1}$ by (15).

Now that we have complete space distributions of u^{n+1}, v^{n+1}, $(\rho')^{n+1}$, and ϕ^{n+1} at $t = t^{n+1}$, the foregoing procedure may be repeated to update the flow field further.

In addition to the equations governing the motion in the interior of the fluid, it is also necessary to specify boundary and initial conditions. Correct treatment of these conditions is of vital importance in the present second-order time scheme.

3. Boundary and Initial Conditions

Consider the situation shown in Fig. 2, i.e., the motion of a stratified fluid in a box with rigid walls. The condition that the normal velocity of the fluid vanish at a rigid wall is met by specifying $u = 0$ along AD and BC, and $v = 0$ along AB and CD. The way variables are defined (Fig. 1) in the present mesh system does not require the knowledge of ρ' or v along AD and BC, nor the specification of u along AB and CD. If ρ' is zero initially along the horizontal rigid boundaries AB and CD, then it remains zero there for all times, according to Eq. (3). Also, we have $\phi_x = 0$ along AD and BC, by applying $u_t = 0$ in Eq. (1). Similarly, $\phi_y = 0$ along AB and CD. These Neumann conditions on ϕ are imposed during the iterative solution of ϕ^{n+1}.

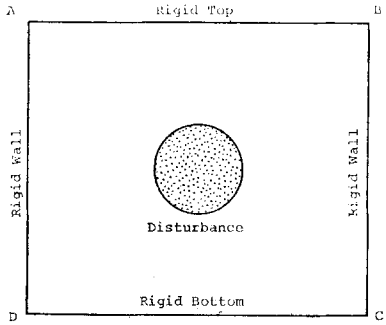

FIG. 2. Rigid boundary conditions.

In the present method it is also necessary to impose boundary conditions on the first temporal derivatives. These are simply: $u_t = 0$ along AD and BC, $v_t = 0$ along AB and CD, $\rho_t' = 0$ along AB and CD if $\rho' = 0$ there initially.

A set of initial values for u, v, ρ', and ϕ are required to begin the numerical integration. These quantities cannot be prescribed arbitrarily. Obviously, the u and v distributions must satisfy the continuity equation (17). Another consistency requirement is more subtle. Suppose the initial velocity field does satisfy the continuity equation and the initial distribution of ρ' is specified. Then, the initial

distribution of the dynamic pressure ϕ cannot be assigned at random. To see this, Eqs. (12) and (14) can be written as

$$\begin{aligned}
(u_t)_{i+(1/2),j} &= A_{i+(1/2),j} - (\phi_{i+1,j} - \phi_{i,j})/\delta x \\
(u_t)_{i-(1/2),j} &= A_{i-(1/2),j} - (\phi_{i,j} - \phi_{i-1,j})/\delta x \\
(v_t)_{i,j+(1/2)} &= B_{i,j+(1/2)} - (\phi_{i,j+1} - \phi_{i,j})/\delta y \\
(v_t)_{i,j-(1/2)} &= B_{i,j-(1/2)} - (\phi_{i,j} - \phi_{i,j-1})/\delta y,
\end{aligned} \tag{20}$$

and, by taking time derivative of each term and applied at the initial instant $t = 0$, Eq. (17) becomes

$$[(u_t)_{i+(1/2),j} - (u_t)_{i-(1/2),j}]/\delta x + [(v_t)_{i,j+(1/2)} - (v_t)_{i,j-(1/2)}]/\delta y = 0. \tag{21}$$

In Eqs. (20), A and B represent those terms that do not involve ϕ, and all the variables are evaluated at $t = 0$. Now, by substituting the expressions (20) into Eq. (21), we have

$$\begin{aligned}
&(\phi_{i+1,j} - 2\phi_{i,j} + \phi_{i-1,j})/(\delta x)^2 + (\phi_{i,j+1} - 2\phi_{i,j} + \phi_{i,j-1})/(\delta y)^2 \\
&\quad = (A_{i+(1/2),j} - A_{i-(1/2),j})/\delta x + (B_{i,j+(1/2)} - B_{i,j-(1/2)})/\delta y
\end{aligned} \tag{22}$$

subject to the boundary conditions: $\phi_x = 0$ on AD and BC and $\phi_y = 0$ on AB and CD. Eq. (22) is, again, a Poisson equation which can be solved by standard procedures to produce the initial ϕ distribution which is *consistent* with the prescribed u, v, and ρ' distributions.

As an example, suppose we choose as initial conditions $u = v = 0$ everywhere in the (x, y) plane, thus satisfying Eq. (17), and $\rho' = 0$ except in the disturbed region (Fig. 2). Then $A \equiv 0$, $B = -(g/\rho^*)\,\rho'$, and the right side of Eq. (22) reduces to

$$-(g/\rho^*)(\rho'_{i,j+(1/2)} - \rho'_{i,j-(1/2)})/\delta y \neq 0$$

which indicates that the initial $\phi \equiv 0$ would be incompatible with the basic governing equations in this case. The consequence of using an inconsistent initial ϕ distribution is the time-splitting behavior of the solution which will be discussed in Section 5.

4. Numerical Stability

A rigorous linear stability analysis has not been performed for the present method. In many applications the velocities u and v associated with the internal waves are so small that the maximum δt is limited by the characteristic time of the problem, i.e., the Brunt–Väisälä period (BV). It has been found that $\delta t = \frac{1}{50}$ BV

gives very satisfactory results. As will be shown shortly, the excellent stability property of the present method is evidenced by the nearly perfect conservation of energy.

5. Sample Calculations

Throughout the present discussion, variables are made dimensionless by the following rules. All lengths are normalized by D, the initial diameter of the disturbed region (Fig. 2). Accelerations are normalized by g, and, consequently, all velocities are measured in terms of $(gD)^{1/2}$. Finally, the density ρ is normalized by ρ^*.

Several numerical experiments have been performed to demonstrate the properties of the present method. Consider a two-dimensional domain consisting of 30×30 cells. As illustrated in Fig. 2, rigid boundaries are used in this example. At $t = 0$ we prescribe the density deviation

$$\rho' = -(\rho_0)_y (y - y_0)\, e^{-0.693(r/r^*)^2} \tag{23}$$

where $(\rho_0)_y = -0.003134$, y_0 is the ordinate of the center of the square domain, r is the radial distance from that center, and $r^* = 0.5$ is the half-strength radius of the disturbed region. The Brunt–Väisälä frequency is $N = (-(g/\rho^*)(\rho_0)_y)^{1/2}$. Also, we take $u = v = 0$ everywhere initially. Because the fluid particles seek their own level in the undisturbed ambient density structure, fluid motions and radiation of internal waves start. When these waves reach the rigid boundaries, complex phenomena of reflection will occur.

The conservation of momentum is guaranteed in the present method, because the convection terms in the momentum equations are written in the flux form. We only have to examine the conservation of mass and energy, which is not obvious from the form of finite-difference equations. The conservation of mass requires

$$\iint \rho'\, dx\, dy = \text{constant} = \iint \rho_0'\, dx\, dy \tag{24}$$

where ρ_0' is ρ' evaluated at $t = 0$, and the double integral covers the entire domain. Thus, the relative error in mass conservation can be defined as

$$\epsilon_\rho = \left| \frac{\iint \rho'\, dx\, dy - \iint \rho_0'\, dx\, dy}{\iint \rho_0(y)\, dx\, dy} \right|. \tag{25}$$

It can be shown [13] that the potential energy in a stratified fluid with constant $(\rho_0)_y$ is given by

$$\text{PE} = \frac{-g}{2(\rho_0)_y} \iint (\rho')^2\, dx\, dy \tag{26}$$

and the kinetic energy is

$$\mathrm{KE} = \tfrac{1}{2}\iint \rho(u^2 + v^2)\, dx\, dy. \tag{27}$$

The total energy TE is the sum of PE and KE. Now we can define the relative error in total energy as

$$\epsilon_{\mathrm{TE}} = \left| \frac{\mathrm{TE} - (\mathrm{TE})_0}{(\mathrm{TE})_0} \right| \tag{28}$$

where $(\mathrm{TE})_0$ is evaluated at $t = 0$.

The computation has been continued for 500 time steps, corresponding to five Brunt–Väisälä periods. The cell size is $\delta x = \delta y = 0.1$ and 0.2 in Cases I and II, respectively, and $\delta t = 1\,\%$ of the Brunt–Väisälä period. In Case II, 60×60 cells are used so that the linear dimension of the computational domain is four times that of Case I. Table I summarizes the relative errors in the conservation laws. Note that even with a poor spatial resolution, such as Case II, the energy conservation has only $0.4\,\%$ maximum error throughout the entire computation. More importantly, this small error in energy does not grow with respect to time; the amplitude of the error can be made smaller by reducing the time step.

TABLE I

	$\delta x, \delta y$	$(\epsilon_\rho)_{\max}$	$(\epsilon_{\mathrm{TE}})_{\max}$
Case I (30×30 cells)	0.10	1.5×10^{-7}	3.5×10^{-3}
Case II (60×60 cells)	0.20	1.5×10^{-7}	4.0×10^{-3}

The effect of using incorrect initial ϕ distribution, which was discussed in Section 3, has also been investigated. The contour plot of the correct initial ϕ-field for Case I, obtained by solving Eq. (22), is shown in Fig. 3. It has been found that if $\phi \equiv 0$ is used as initial condition, which is incompatible with the other initial conditions, namely, $u = v = 0$ and $\rho' \neq 0$, then a noticeable oscillation between time steps occurs in the solution, particularly in the total energy. Time-splitting error does not arise when the correct initial ϕ is used.

It is quite interesting to see how the partition between kinetic and potential energies evolves in an inviscid stratified fluid with initial disturbance described by Eq. (23). Consider Case I where the size of computation domain is only 3×3. At $t = 0$, the total energy consists entirely of the potential energy, because $u = v = 0$. As the fluid particles return to their own density levels, motion starts and some

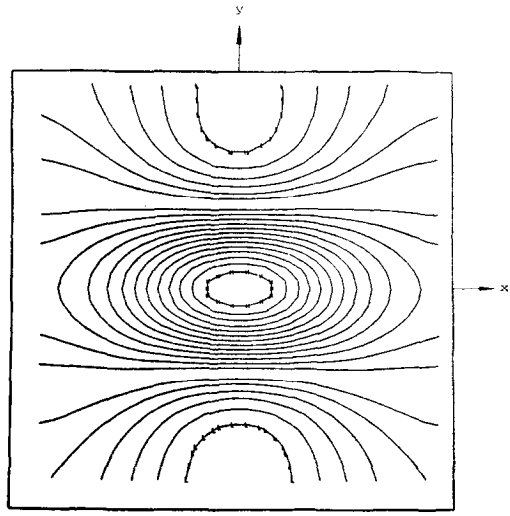

FIG. 3. Contours of ϕ-field at $t = 0$ for Case I. The symbol H represents $\phi = 0.002985$ and L represents $\phi = -0.001514$. The contour interval is $\Delta\phi = 0.000214$.

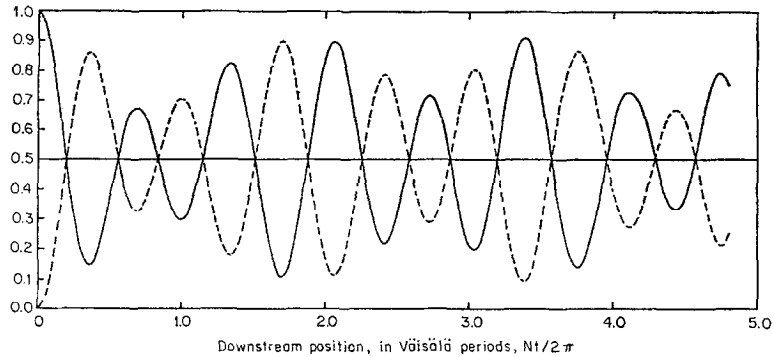

FIG. 4. Energy partition for case I. The solid line indicates the potential energy divided by the total energy, while the dash line is the kinetic energy divided by the total energy.

of the potential energy is converted into kinetic energy. Figure 4 shows the time history of energy partition. Equal partition of energy is quite evident even though wall reflections severely interfere with the flow field. In Case II, where the computational domain is considerably larger, the effect of wall reflections is delayed. Again, as shown in Fig. 5, equal partition of energy is found. Moreover, because of the absence of reflections at early times the pattern of the energy curves in this case is very different from that of Case I.

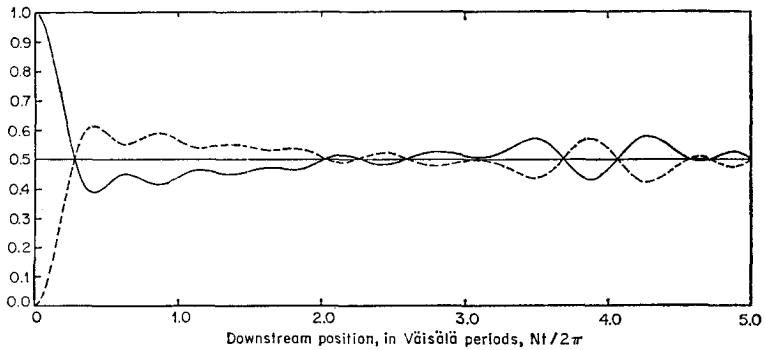

FIG. 5. Energy partition for case II. The solid line indicates the potential energy divided by the total energy, while the dash line is the kinetic energy divided by the total energy.

6. CONCLUSIONS

An explicit, second-order, numerical, time integration method for calculating the motion of an incompressible, stratified fluid has been developed. It has been demonstrated that this method is stable for long-term integration with respect to time and that mass, momentum, and energy are very well conserved. Moreover, the small error in the total energy is nonaccumulative.

ACKNOWLEDGMENTS

This work was carried out in the main while the author was on the professional staff of Science Applications, Inc., La Jolla, California. The research was sponsored by Applied Physics Laboratory, the Johns Hopkins University, as a part of the work supported by the U. S. Navy Contract N00017-72-C-4401.

REFERENCES

1. A. ARAKAWA, *J. Comput. Phys.* **1** (1966), 119–143.
2. K. BRYAN, *Mon. Weather Rev.* **94** (1966), 39–40.
3. G. P. WILLIAMS, *J. Fluid Mech.* **37** (1969), 727–750.
4. S. A. PIACSEK AND G. P. WILLIAMS, *J. Comput. Phys.* **6** (1970), 392–405.
5. S. A. ORSZAG AND M. ISRAELI, *Ann. Rev. Fluid Mech.* **6** (1974), 281–318.
6. H. O. KREISS AND J. OLIGER, *Tellus* **24** (1972).
7. J. P. DUGAN, A. C. WARN-VARNAS, AND S. A. PIACSEK, Numerical Model for Mixed Region Collapse in a Stratified Fluid, Naval Research Laboratory Memorandum Report 2597, Naval Research Laboratory, Washington, D. C., 1973.
8. P. J. ROACHE, "Computational Fluid Dynamics," pp. 59–60. Hermosa Publishers, Albuquerque, New Mexico, 1972.

9. P. D. POLGER, A Study of Nonlinear Computational Instability for a Two-Dimensional Model, NOAA TM NWS NMC-49, U. S. Department of Commerce, National Oceanic and Atmospheric Administration, Washington, D. C., 1971.
10. J. S. TURNER, "Buoyancy Effects in Fluids," pp. 6–9. Cambridge University Press, Cambridge, 1973.
11. J. GAZDAG, *J. Comput. Phys.* **13** (1973), 100–113.
12. F. H. HARLOW AND J. E. WELCH, *Phys. Fluids* **8** (1965), 2182.
13. J. H. STUHMILLER AND R. K. -C. CHAN, Potential Energy in a Stratified Fluid, to appear.